mathematics

MDPI

Article

Stochastic Model of Virus–Endosome Fusion and Endosomal Escape of pH-Responsive Nanoparticles

Sergei Fedotov [1,*], Dmitri Alexandrov [2], Ilya Starodumov [2] and Nickolay Korabel [1,*]

[1] Department of Mathematics, The University of Manchester, Manchester M13 9PL, UK
[2] Laboratory of Multi-Scale Mathematical Modeling, Department of Theoretical and Mathematical Physics, Ural Federal University, Lenin Ave., 51, 620000 Ekaterinburg, Russia; dmitri.alexandrov@urfu.ru (D.A.); ilyastarodumov@yahoo.ca (I.S.)
* Correspondence: sergei.fedotov@manchester.ac.uk (S.F.); nickolay.korabel@manchester.ac.uk (N.K.)

Abstract: In this paper, we set up a stochastic model for the dynamics of active Rab5 and Rab7 proteins on the surface of endosomes and the acidification process that govern the virus–endosome fusion and endosomal escape of pH-responsive nanoparticles. We employ a well-known cut-off switch model for Rab5 to Rab7 conversion dynamics and consider two random terms: white Gaussian and Poisson noises with zero mean. We derive the governing equations for the joint probability density function for the endosomal pH, Rab5 and Rab7 proteins. We obtain numerically the marginal density describing random fluctuations of endosomal pH. We calculate the probability of having a pH level inside the endosome below a critical threshold and therefore the percentage of viruses and pH-responsive nanoparticles escaping endosomes. Our results are in good qualitative agreement with experimental data on viral escape.

Keywords: stochastic ODE's; virus–endosome fusion; endosomal escape; viruses; pH-responsive nanoparticles

Citation: Fedotov, S.; Alexandrov, D.; Starodumov, I.; Korabel, N. Stochastic Model of Virus–Endosome Fusion and Endosomal Escape of pH-Responsive Nanoparticles. *Mathematics* **2022**, *10*, 375. https://doi.org/10.3390/math10030375

Academic Editor: Giancarlo Consolo

Received: 30 December 2021
Accepted: 24 January 2022
Published: 26 January 2022

1. Introduction

Viruses use diverse processes to enter the host cell: some undergo membrane fusion and deliver genetic material directly into the cytoplasm; others use an endocytic pathway by hijacking endosomes and exploit the intracellular transport along microtubules to deliver a viral genome to sites of replication [1,2]. To avoid lysosomal degradation, viruses must escape from endosomes into the cytoplasm. This escape is mediated by the fusion of the endosomal and virus membrane that depends on conformational change of the viral glycoprotein hemagglutinin triggered by lowered pH [3–5]. Therefore, the stochastic residence time of the virus inside endosomes depends on the endosomal acidification process. A typical cytoplasmic pH is around 7.0, which drops to around pH 6.4 in early endosomes and further to around pH 5.0 in lysosomes. The maturation of early endosomes (EE) to late endosomes (LE) is governed by the conversion of Rab5 to Rab7 and is simultaneously followed by acidification [6,7]. The low internal pH of these membrane-bound vesicles is sustained by the active ATP-dependent proton pumps on their membranes. These key proteins on the surface of endosomes are the main factors in the identification of early and late endosomes, their biogenesis and fusion/fission processes [8]. Rab5 proteins mark early endosomes, whereas Rab7 proteins are localized to late endosomes and lysosomes.

Various adenovirus-based vectors and lipid nanoparticles (LNPs) have been used as a platform for gene delivery with the purpose of treating human disorders [9]. However, their limited ability to perform endosomal escape seriously restricts their use as delivery vehicles since only a small percentage of genetic material can escape endosomes and enter the cell's cytoplasm [10,11]. Currently, lipid nanoparticles represent the most effective tool for genetic material delivery [12]. After successful endocytosis, the internalized LNPs are usually trapped in endosomes and advanced to the lysosomes for degradation. Therefore,

endosomal escape before lysosomal degradation is a crucial process for successful delivery of site-specific drugs. In recent years, stimuli-responsive nanoparticles triggered by low pH in endosomes have attracted much attention regarding the problem of targeted drug delivery [13]. It has been shown that pH-responsive nanoparticles have the potential to facilitate therapeutics delivery by effective escape from endosomes before degradation [14–17]. Therefore, for viruses and lipid nanoparticles, escaping from the endosome and entering the cytoplasm is the only avenue for replication as lysosomal degradation, which occurs after endosome maturation, will render the genetic material within these vessels useless.

Several mathematical models have been developed to describe the transition from early to late endosomes controlled by a mechanism called Rab-conversion. Del Conte-Zerial et al. [18] set up a variety of models including a 'cut-off switch' model to explain a fast initial growth of Rab5 proteins and their sudden removal during Rab5 to Rab7 conversion. A system of four nonlinear differential equations describes the dynamics of active and inactive Rab5 and Rab7 proteins. This nonlinear model is concerned with the kinetics of how Rab5 activates Rab7, which takes over and suppresses Rab5 through a negative feedback loop. Another interesting development is a mathematical model involving the coupling of the density of Rab5 on a single endosome and the average number of endosomes inside cells [8]. Zeigerer et al. demonstrated both theoretically and experimentally that Rab5 coordinates endosomes by regulating their number and size. Using a nonlinear dynamical system for active/inactive Rab5 proteins, they implemented the impact of fusion and fission events on Rab5 dynamics in terms of the mean number of endosomes inside the cell. Recently, a Smoluchowskii-like equation has been suggested [19] to describe the stochastic dynamics of the number of endosomes inside the cell, as well as the mean/standard deviation of active Rab5 and Rab7 proteins. Using the relationship between Rab5/Rab7 densities and endosomal pH, they have analyzed the variability of viral escape times.

The purpose of this paper is to set up a simple stochastic model describing the endosomal escape of viruses and pH-responsive nanoparticles. An illustration of the simplified endocytic pathway, which we employ, is shown in Figure 1. The main idea is to analyze the stochastic acidification process and endosomal escape in terms of random dynamics of Rab5 to Rab7 conversion described by stochastic differential equations. The aim is to obtain the joint probability density function for the endosomal pH, and the number of Rab5 and Rab7 proteins, and therefore calculate the probability of having a pH level inside an endosome below a critical threshold. This probability can be interpreted as a percentage of viruses and pH-responsive nanoparticles escaping endosomes [19].

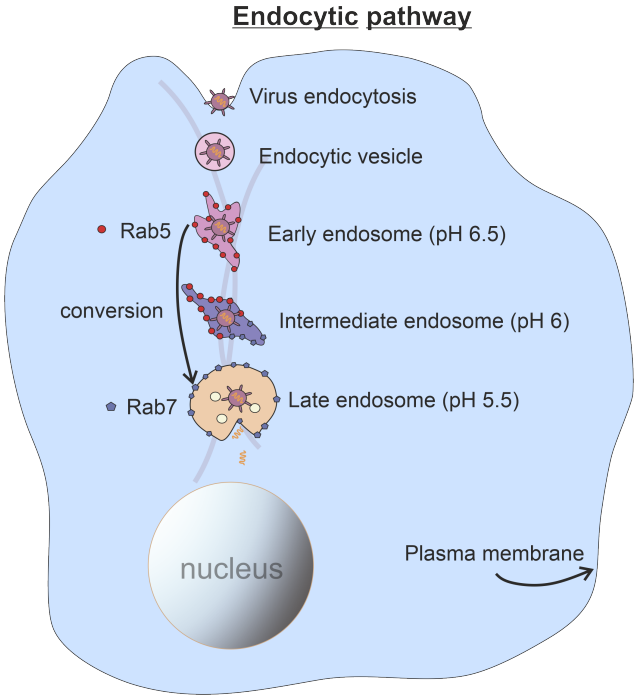

Figure 1. A schematic illustration of the endocytic pathway: a virus entering the cell via endocytosis is transported inside the endocytic vesicle and early endosomes towards intermediate and late endosomes. The acidification of endosomes and the pH-dependent release of viral genetic material into the cytoplasm after the late endosome's membrane rupture are mediated by the conversion of Rab5/Rab7 proteins on the endosome surface.

2. Stochastic Model for Rab5 to Rab7 Conversion

To describe Rab5 to Rab7 conversion, we employ a cut-off switch model [18] and use its linearized version [19]. Rink et al. [6] found that the concentration of Rab5 molecules exhibits very strong fluctuations in single early endosomes. To describe these random fluctuations, we add the stochastic terms such that the simplified dynamics of active Rab5 and Rab7 proteins can be described by the following stochastic differential equations:

$$\begin{aligned} \frac{dR_5}{dt} &= -\nu_{55}R_5 - \nu_{57}R_7 + \nu_{50}N(t) + \xi_5(t), \\ \frac{dR_7}{dt} &= \nu_{75}R_5 - \nu_{77}R_7 + \nu_{70}N(t) + \xi_7(t), \end{aligned} \tag{1}$$

where $R_5(t)$ and $R_7(t)$ are the number of active Rab5 and Rab7 per endosome, $N(t)$ is the average number of endosomes in the cell, $\xi_5(t)$ and $\xi_7(t)$ are the random noise terms with zero means. There are six rate constants in the dynamical system (1), and their values have been estimated in [19]. Specifically, ν_{75} is the rate of the gradual activation of Rab7 by Rab5, while ν_{57} gives the rate of inactivation of Rab5 by Rab7; ν_{55} and ν_{77} are the rates of self-inactivation mechanisms of Rab5 and Rab7; ν_{50} and ν_{70} describe the rates of Rab5 and Rab7 activation process that depends on the average number of endosomes in cell, N(t) (see details in [19]).

We introduce the noise terms $\xi_5(t)$ and $\xi_7(t)$ because experimental knowledge is yet to decipher the multitude of mechanisms that are responsible for random endosome evolution and dynamics of Rab5, Rab7 and pH value within the cell. With the cell being a system in non-equilibrium, we account for multiple stochastic processes in cells using white Gaussian and Poisson noises. Moreover, multiple stochastic mechanisms contribute to cell-to-cell variability in viruses and nanoparticle uptake [20–22], so considering variability in initial conditions could be another study. In particular, for each early endosome, one can consider random initial numbers of Rab5 and Rab7 as well as pH value.

We should emphasize that the linearization of nonlinear equations [18] for Rab5 and Rab7 facilitates analytical approaches to solutions without sacrificing the qualitative model behavior. For example, without the noise, Equation (1) can be solved analytically (see the Appendix A). Incorporating nonlinear kinetic terms may introduce problems such as hyper-parameter tuning and greater sensitivity, which make stochastic numerical algorithms difficult to verify. Exploring these non-linearities and their interaction with noise terms would be the subject of future studies.

The relaxation equation for the endosomal pH, $p_H(t)$, can be written as:

$$\frac{dp_H(t)}{dt} = -\frac{p_H(t) - p_H^s(R_5, R_7)}{\tau_H}, \tag{2}$$

where $p_H^s(R_5, R_7)$ is the steady endosomal pH, τ_H is the relaxation constant. The relationship between the level of active Rab5/Rab7 proteins and $p_H^s(t)$ can be approximated by [5]:

$$p_H^s(R_5, R_7) = p_H^e + (p_H^l - p_H^e)\frac{R_7(t)}{R_5(t) + R_7(t)}. \tag{3}$$

In Equation (3), the constants p_H^e and p_H^l give the endosomal pH in early endosomes and late endosomes/lysosomes correspondingly.

In this paper, we consider two cases for the random noise terms $\xi_i(t)$:
(1) *the white Gaussian noise* with zero mean

$$\xi_i(t) = \sqrt{2D_i}\frac{dW_i(t)}{dt}, \quad i = 5, 7, \tag{4}$$

where $W_5(t)$ and $W_7(t)$ are independent standard Wiener processes and D_i are diffusion coefficients;
(2) *the white Poisson noise* with zero mean:

$$\xi_i(t) = \sum_{k=1}^{n_i(t)} \xi_k \delta(t - t_k), \quad i = 5, 7, \tag{5}$$

where $n_i(t)$ is the Poisson process with the rate λ_i. The random amplitudes ξ_k are distributed with the density $f_i(x)$ with zero mean. One of the reasons why we employ Poisson noise is that it is more biologically relevant as it generates jumps in values of Rab5 and Rab7. These jumps emulate the fusion and fission of endosomes, which create discontinuous jumps in the number of Rab5 and Rab7. In what follows we will show that, for Poisson noise, the tails of the pH probability density are longer than those predicted for the Gaussian noise. It has been also observed [23] that Rab5-positive early endosomes carrying viruses mature either through progressive appearance of Rab7 proteins (55%) or by jumps in Rab7 involving fusion with Rab7-positive late endosome (45%). In ref. [19], the Smoluchowskii equation has been employed to describe the stochastic fusion/fission dynamics of endosomes inside cells. Although this formulation is theoretically attractive, the model's non-linearities make it difficult to analyze and so we propose Poisson noise as a simpler method to model stochastic endosome fusion/fission, which leads to jumps in internal pH, and the number of Rab5 and Rab7.

We introduce the joint probability density function $\rho(p_H, R_5, R_7, t)$ for the endosomal pH and the random Rab5 and Rab7 proteins. It follows from Equations (1)–(5) that it obeys the governing equation

$$\begin{aligned}\frac{\partial \rho}{\partial t} &= \frac{\partial}{\partial p_H}\left[\frac{p_H - p_H^s}{\tau_H}\rho\right] + \frac{\partial}{\partial R_5}[(\nu_{55}R_5 + \nu_{57}R_7 - \nu_{50}N(t))\rho] \\ &+ \frac{\partial}{\partial R_7}[(-\nu_{75}R_5 + \nu_{77}R_7 - \nu_{70}N(t))\rho] + L_5\rho + L_7\rho.\end{aligned} \tag{6}$$

Here, the operators $L_i\rho$ have the following forms:
(1) for the white Gaussian noise [24]

$$L_i\rho = D_i \frac{\partial^2 \rho}{\partial R_i^2}; \quad i = 5, 7 \tag{7}$$

(2) for the white Poisson noise [24]

$$\begin{aligned} L_5\rho &= \lambda_5 \int_0^\infty \rho(p_H, R_5 - x, R_7, t) f_5(x) dx - \lambda_5 \rho, \\ L_7\rho &= \lambda_7 \int_0^\infty \rho(p_H, R_5, R_7 - x, t) f_7(x) dx - \lambda_7 \rho. \end{aligned} \tag{8}$$

The average number of endosomes $N(t)$ obeys the equation [8]

$$\frac{dN(t)}{dt} = \lambda + k_{fis} N(t) - k_{fus} N^2(t), \tag{9}$$

where k_{fis} and k_{fus} are endosome fission and fusion rates, λ is positive constant describing the production of endosomes with dimensions of number of endosomes per unit time. An exact solution of Equation (9) with zero initial condition ($N(0) = 0$) reads as

$$N(t) = \frac{k_{fis}}{2k_{fus}} + \frac{\gamma(t) - 1}{\gamma(t) + 1} b, \; \gamma(t) = \frac{b + x_0}{b - x_0} e^{2bk_{fus}t} \tag{10}$$

with

$$b = \frac{1}{2k_{fus}} \sqrt{k_{fis}^2 + 4k_{fus}\lambda}, \; x_0 = -\frac{k_{fis}}{2k_{fus}}. \tag{11}$$

From (10) one can obtain the steady-state solution

$$N_s = \frac{k_{fis}}{2k_{fus}} + b. \tag{12}$$

3. Endosomal Escape

In this section, we consider the problem of virus escape from the endosome triggered by low pH. To deliver genetic materials to cytoplasm, viruses developed a sophisticated mechanism for escape from endosomes and avoid degradation in lysosomes. For the most endocytosed viruses, a major factor for their endosomal escape is the strong pH dependence of the viral fusion with endosome membrane. This dependence greatly varies among viruses [4]: those with high (pH around 6) pH dependencies such as SFV 41, VSV 42, fuse in early endosomes, whereas those with lower pH dependencies (pH around 5), such as influenza viruses, fuse in late endosomes. A detailed model of escape from endosomes involving conformational change of the viral glycoprotein hemagglutinin induced by low pH was developed in [5]. In recent work [19], the authors suggested a brilliant idea that random fluctuations of Rab5 and Rab7 proteins could explain the variability of pH-driven endosomal escape. They assumed that the fluctuations of endosomal pH can be described by a normal distribution: $pH(t) \sim \mathcal{N}[\overline{pH}(t), \sigma_{pH}(t)]$. It allows the calculation of the probability of having a pH level below a critical threshold. This probability can be interpreted as the normalized number of viral escape events [19].

Here, we assume that low pH is sufficient to trigger endosomal escape of the viruses and pH-responsive nanoparticles. The random fluctuations of endosomal pH is described by the marginal density

$$\rho(p_H, t) = \int \int \rho(p_H, R_5, R_7, t) dR_5 dR_7. \tag{13}$$

This function gives the probability of virus-carrying endosomes having a given p_H. It is difficult to calculate this density analytically; therefore, in what follows we present the results of our Monte Carlo simulations of endosomal pH density, $\rho(p_H, t)$. The values of parameters which were used in our numerical simulations are given in Table 1, based on ref. [19].

Table 1. Parameters used in numerical simulations.

Parameter	Value	Units	Parameter	Value	Units
k_{fis}	4.54	s^{-1}	ν_{55}	0.0062	s^{-1}
k_{fus}	0.0032	s^{-1}	ν_{70}	1.2×10^{-6}	s^{-1}
ν_{50}	1.3×10^{-5}	s^{-1}	λ	0.4389	s^{-1}
ν_{57}	0.0040	s^{-1}	p_H^e	6	-
ν_{77}	0.0013	s^{-1}	p_H^l	4.5	-
ν_{75}	0.0032	s^{-1}	τ_H	0.01	s

4. Numerical Simulations and Results

Numerical simulations of (1) were performed in Wolfram Mathematica. The built-in tools for the Itô stochastic differential equations were used to numerically solve the system of Equation (1) with the white Gaussian noise. To simulate the white Poisson noise (5), random jump times were chosen using a random generator with Poisson distribution. We used uniform density functions $f_i(x)$ $(i = 5, 7)$ (see the discussion after Equation (5)) for the random amplitudes ξ_k, $f_i(x) = 1/(2A_i)$ on $[-A_i, A_i]$. The system of stochastic differential Equation (1) was solved using the NDSolve function. The results of numerical simulations are shown in Figures 2–4 for different parameters of noise (see figures captions). Histograms (Figure 3) were plotted based on 300 sample paths.

To make a comparative analysis of the effects of different noises on the distribution of pH inside endosomes, we assume that the diffusive coefficients of Gaussian noise D_i are equal to diffusion coefficients of Poisson noise $\lambda_i < x_i^2 > /2$ that is $D_i = \lambda_i < x_i^2 > /2$, where $x_i^2 = \int x^2 f_i(x) dx$. In particular, for uniform density we have $< x_i^2 >= A_i^2/3$ and therefore $D_i = \lambda_i A_i^2/6$.

The stochastic time evolution of $R_5(t)$ and $R_7(t)$ shows the initial faster growth of Rab5 compared to Rab7 (Figure 2). At later times, Rab7 takes over and suppresses Rab5. As a result of random fluctuations of Rab5 and Rab7, endosomes are characterized by distributions of pH values. We compare the distributions of pH values calculated at different times (see Figure 3). These distributions are broad, which supports the variability of experimentally observed pH values. However, we find that for Poisson noise, the distribution tails are longer, which produces more dispersed pH values compared to Gaussian noise at all times. For times $t < 400$ s, this gives more endosomes with small pH values compared to Gaussian noise.

In Figure 4 we compare the time dependence of the fraction of endosomes $R(t)$ with pH < 5.2 and the time behavior of the average <pH>. For times $t < 400$ s, $R(t)$ for Poisson noise is greater than $R(t)$ for Gaussian noise. At $t \simeq 500$ s, $R(t)$ approaches $\simeq 0.9$–0.95 for Poisson noise and Gaussian noise. We found that compared to Gaussian noise, Poisson noise produces more heterogeneous times of viruses pH-triggered escape out of endosomes especially at small time ($t < 400$ s). This is in qualitative agreement with the experimental observation of the variability of escape times of Dengue virus. Therefore, we suggest that Poisson noise is more realistic for stochastic modeling of virus–endosome fusion and endosomal escape.

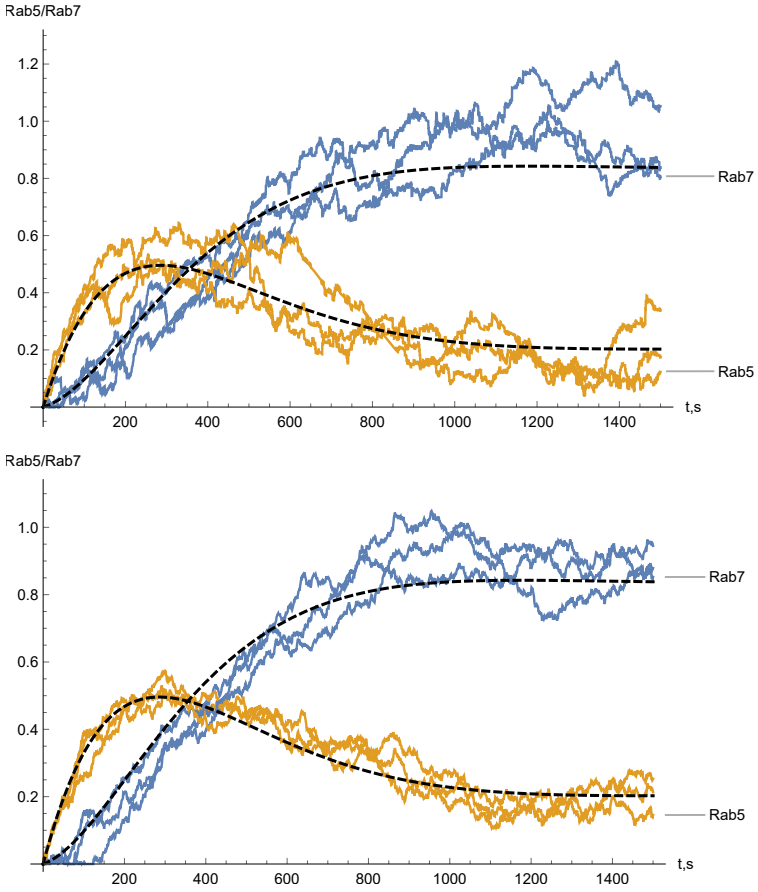

Figure 2. Results of numerical integration of Equations (1) and (9) for Poisson noise with uniform density $f_i(x) = \frac{1}{2A_i}$ on $[-A_i, A_i]$, $i = 5,7$, $A_5 = A_7 = 0.01$, $\lambda_5 = \lambda_7 = 1$ (top panel) and Gaussian noise with $D_5 = D_7 = \frac{1}{6} \cdot 10^{-5}$ (bottom panel). The dashed lines represent the solutions without the noise.

In [23], the typical timescale for virus escape has been described as follows. Within a few seconds post-binding, the virus progresses towards an intermediate endosome that matures into a Rab7-positive late endosome. At 508 s post-infection the virus escapes this organelle. This agrees with our simulation results of the fraction of endosomes $R(t)$ with pH < 5.2 which at 500 s approach 1.

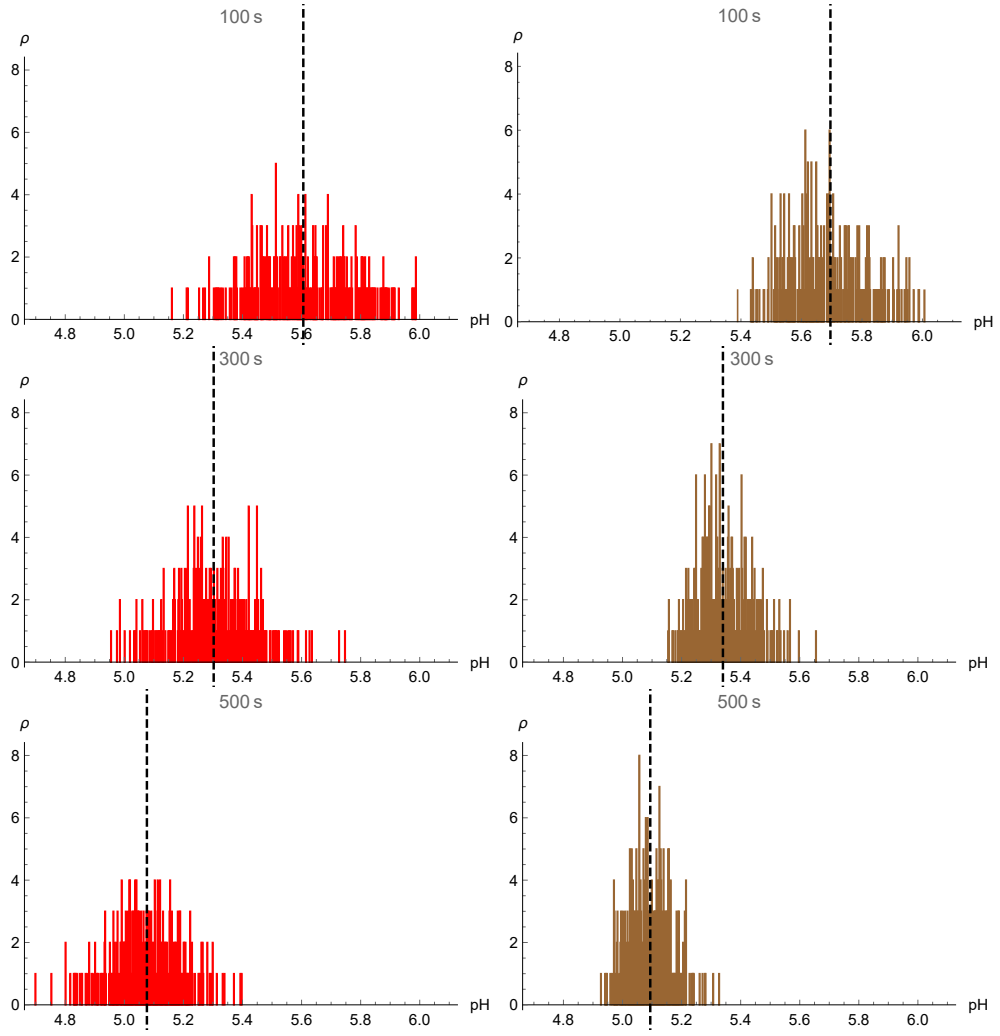

Figure 3. Histograms for $\rho(p_H, t)$ (Equation (13)) after numerical integration of Equations (1), (2) and (9) for Poisson (left panels) and Gaussian (right panels) noises with the parameters presented in Figure 2. Rows show the distribution of pH values calculated at different times $t = 100$ s, $t = 300$ s, and $t = 500$ s. Dashed lines show the mean values.

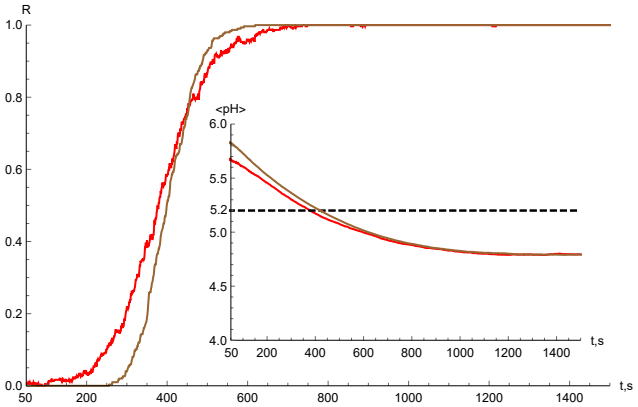

Figure 4. Results of numerical integration of Equations (1), (2) and (9) for Poisson (red lines) and Gaussian (brown lines) noises with the parameters presented in Figure 2. Here we show the time dependence of the fraction of endosomes $R(t)$ with pH$<$ 5.2 and the time behavior of the average <pH>.

5. Discussion

We have presented the stochastic model for the random dynamics of active Rab5 and Rab7 proteins on the surface of endosomes together with endosomal acidification process. The fluctuating low pH triggers the random virus–endosome fusion that determines the delivery of viral genome into the cytoplasm. The same random acidification process governs endosomal escape of pH-responsive nanoparticles. We have employed the so-called "cut-off switch" model [18,19] for Rab5 to Rab7 conversion and consider two sources of randomness separately: white Gaussian noise and white Poisson noise both with zero mean. We have obtained the governing equations for the joint probability density function for the endosomal pH, Rab5 and Rab7 proteins. We have calculated the marginal density of endosomal pH, $\rho(p_H, t)$, the probability of having a pH level inside endosome below a critical threshold, and therefore the percentage of viruses and pH-responsive nanoparticles escaping endosomes. The outcome of our simplified mathematical model qualitatively supports well-known experimental data of great variability of endosomal escape times. For example, the majority (80%) of Dengue virus escape from Rab7-positive late endosomes without Rab5 proteins, 15% of the viruses leave Rab5/Rab7 intermediate endosomes, and 5% of the viruses escape from Rab5-positive early endosomes without Rab7 [23]. The typical timescale for virus escape agrees well with the timescale found in simulations when the fraction of endosomes with pH < 5.2 approach 1.

Our results can be extended in several ways. For example, one can take into account multiplicative noises that might lead to noise-induced transitions [25] for a nonlinear cut-off switch model [18]. It would be interesting to take into account the stochastic anomalous intracellular transport of viruses and nanoparticles along microtubules to the perinuclear region [26–29]. Certainly, the anomalous endosomal movements have implications on their fusion and fission inside cells and therefore Rab5 to Rab7 conversion. We are planning to consider the impact of the anomalous dynamics in the future work. It is also interesting to consider structural changes in the microtubule network induced by invading viruses [30] as well as the topology of microtubular network [31]. Our model opens new avenues for the quantitative analysis of the endosomal escape of a virus-mimicking pH-responsive nanoparticle for anti-tumor therapeutics delivery [32–35].

Author Contributions: Conceptualization, S.F. and D.A.; methodology, S.F.; software, I.S.; validation, I.S. and N.K.; formal analysis, D.A.; investigation, S.F. and D.A; resources, S.F., D.A. and N.K.; writing—original draft preparation, S.F.; writing—review and editing, S.F., D.A. and N.K; visualization, I.S. and N.K; supervision, S.F.; project administration, S.F.; funding acquisition, S.F, D.A. and N.K. All authors have read and agreed to the published version of the manuscript.

Funding: S.F. and N.K. were funded by EPSRC Grant No. EP/V008641/1. D.A. and I.S. were funded by the Ministry of Science and Higher Education of the Russian Federation (Project No. 075-15-2021-1002).

Institutional Review Board Statement: Not applicable.

Informed Consent Statement: Not applicable.

Data Availability Statement: Data are contained within the article.

Acknowledgments: We thank Daniel Han for valuable discussions and reading the manuscript.

Conflicts of Interest: The authors declare no conflict of interest.

Appendix A

Here we present an exact analytical solution for the levels of Rab5 and Rab7 proteins without the noise (see Equation (1))

$$R_5(t) = \frac{1}{\nu_{75}}\left(\frac{dR_7}{dt} - \nu_{70}N(t) + \nu_{77}R_7(t)\right),$$
$$R_7(t) = \frac{1}{\alpha_1 - \alpha_2}\int_0^t g(\tau)[\exp(\alpha_1(t-\tau)) - \exp(\alpha_2(t-\tau))]d\tau, \quad \text{(A1)}$$

where

$$g(t) = (\nu_{70}\nu_{55} + \nu_{75}\nu_{50})N(t) + \nu_{70}\frac{dN(t)}{dt},$$
$$\alpha_{1,2} = \frac{-\alpha \pm \sqrt{\alpha^2 - 4\beta}}{2},\ \beta = \nu_{57}\nu_{75} + \nu_{55}\nu_{77},\ \alpha = \nu_{77} + \nu_{55},$$

and $R_5(0) = R_7(0) = 0$.

References

1. Mercer, J.; Schelhaas, M.; Helenius, A. Virus entry by endocytosis. *Annu. Rev. Biochem.* **2010**, *79*, 803–833. [CrossRef] [PubMed]
2. Staring, J.; Raaben, M.; Brummelkamp, T.R. Viral escape from endosomes and host detection at a glance. *J. Cell Sci.* **2018**, *131*, jcs216259. [CrossRef] [PubMed]
3. Lagache, T.; Danos, O.; Holcman, D. Modeling the step of endosomal escape during cell infection by a nonenveloped virus. *Biophys. J.* **2012**, *102*, 980–989. [CrossRef] [PubMed]
4. White, J.M.; Whittaker, G.R. Fusion of enveloped viruses in endosomes. *Traffic* **2016**, *17*, 593–614. [CrossRef]
5. Lagache, T.; Sieben, C.; Meyer, T.; Herrmann, A.; Holcman, D. Stochastic model of acidification, activation of hemagglutinin and escape of influenza viruses from an endosome. *Front. Phys.* **2017**, *5*, 25. [CrossRef]
6. Rink, J.; Ghigo, E.; Kalaidzidis, Y.; Zerial, M. Rab conversion as a mechanism of progression from early to late endosomes. *Cell* **2005**, *122*, 735–749. [CrossRef]
7. Poteryaev, D.; Datta, S.; Ackema, K.; Zerial, M.; Spang, A. Identification of the switch in early-to-late endosome transition. *Cell* **2010**, *141*, 497–508. [CrossRef]
8. Zeigerer, A.; Gilleron, J.; Bogorad, R.L.; Marsico, G.; Nonaka, H.; Seifert, S.; Epstein-Barash, H.; Kuchimanchi, S.; Peng, C.G.; Ruda, V.M.; et al. Rab5 is necessary for the biogenesis of the endolysosomal system in vivo. *Nature* **2012**, *485*, 465–470. [CrossRef]
9. Wang, D.; Tai, P.W.; Gao, G. Adeno-associated virus vector as a platform for gene therapy delivery. *Nat. Rev. Drug Discov.* **2019**, *18*, 358–378. [CrossRef]
10. Sahay, G.; Querbes, W.; Alabi, C.; Eltoukhy, A.; Sarkar, S.; Zurenko, C.; Karagiannis, E.; Love, K.; Chen, D.; Zoncu, R.; et al. Efficiency of siRNA delivery by lipid nanoparticles is limited by endocytic recycling. *Nat. Biotechnol.* **2013**, *31*, 653–658. [CrossRef]
11. Maugeri, M.; Nawaz, M.; Papadimitriou, A.; Angerfors, A.; Camponeschi, A.; Na, M.; Hölttä, M.; Skantze, P.; Johansson, S.; Sundqvist, M.; et al. Linkage between endosomal escape of LNP-mRNA and loading into EVs for transport to other cells. *Nat. Commun.* **2019**, *10*, 4333. [CrossRef] [PubMed]
12. Gilleron, J.; Querbes, W.; Zeigerer, A.; Borodovsky, A.; Marsico, G.; Schubert, U.; Manygoats, K.; Seifert, S.; Andree, C.; Stöter, M.; et al. Image-based analysis of lipid nanoparticle–mediated siRNA delivery, intracellular trafficking and endosomal escape. *Nat. Biotechnol.* **2013**, *31*, 638–646. [CrossRef]
13. Zhou, K.; Wang, Y.; Huang, X.; Luby-Phelps, K.; Sumer, B.D.; Gao, J. Tunable, Ultrasensitive pH-Responsive Nanoparticles Targeting Specific Endocytic Organelles in Living Cells. *Angew. Chem. Int. Ed.* **2011**, *50*, 6109–6114. [CrossRef] [PubMed]
14. Selby, L.I.; Cortez-Jugo, C.M.; Such, G.K.; Johnston, A.P. Nanoescapology: Progress toward understanding the endosomal escape of polymeric nanoparticles. *Wiley Interdiscip. Rev. Nanomed. Nanobiotechnol.* **2017**, *9*, e1452. [CrossRef] [PubMed]
15. Kongkatigumjorn, N.; Smith, S.A.; Chen, M.; Fang, K.; Yang, S.; Gillies, E.R.; Johnston, A.P.; Such, G.K. Controlling endosomal escape using pH-responsive nanoparticles with tunable disassembly. *ACS Appl. Nano Mater.* **2018**, *1*, 3164–3173. [CrossRef]
16. Deirram, N.; Zhang, C.; Kermaniyan, S.S.; Johnston, A.P.; Such, G.K. pH-responsive polymer nanoparticles for drug delivery. *Macromol. Rapid Commun.* **2019**, *40*, 1800917. [CrossRef]
17. Andrian, T.; Riera, R.; Pujals, S.; Albertazzi, L. Nanoscopy for endosomal escape quantification. *Nanoscale Adv.* **2021**, *3*, 10–23. [CrossRef]
18. Del Conte-Zerial, P.; Brusch, L.; Rink, J.C.; Collinet, C.; Kalaidzidis, Y.; Zerial, M.; Deutsch, A. Membrane identity and GTPase cascades regulated by toggle and cut-out switches. *Mol. Syst. Biol.* **2008**, *4*, 206. [CrossRef]
19. Castro, M.; Lythe, G.; Smit, J.; Molina-París, C. Fusion and fission events regulate endosome maturation and viral escape. *Sci. Rep.* **2021**, *11*, 7845. [CrossRef]
20. Katsnelson, B.; Privalova, L.; Sutunkova, M.; Khodos, M.; Shur, V.Y.; Shishkina, E.; Tulakina, L.; Pichugova, S.; Beikin, J. Uptake of some metallic nanoparticles by, and their impact on pulmonary macrophages in vivo as viewed by optical, atomic force, and transmission electron microscopy. *J. Nanomed. Nanotechnol.* **2012**, *3*, 1–8. [CrossRef]
21. Rees, P.; Wills, J.W.; Brown, M.R.; Barnes, C.M.; Summers, H.D. The origin of heterogeneous nanoparticle uptake by cells. *Nat. Commun.* **2019**, *10*, 2341. [CrossRef] [PubMed]

22. Åberg, C.; Piattelli, V.; Montizaan, D.; Salvati, A. Sources of variability in nanoparticle uptake by cells. *Nanoscale* **2021**, *13*, 17530–17546. [CrossRef] [PubMed]
23. Van Der Schaar, H.M.; Rust, M.J.; Chen, C.; van der Ende-Metselaar, H.; Wilschut, J.; Zhuang, X.; Smit, J.M. Dissecting the cell entry pathway of dengue virus by single-particle tracking in living cells. *PLoS Pathog.* **2008**, *4*, e1000244. [CrossRef]
24. Gardiner, C.W. *Handbook of Stochastic Methods*; Springer: Berlin, Germany, 1985; Volume 3.
25. Horsthemke, W.; Lefever, R. Noise-induced transitions in physics, chemistry, and biology. In *Noise-Induced Transitions: Theory and Applications in Physics, Chemistry, and Biology*; Springer: Berlin/Heidelberg, Germany, 1984; pp. 164–200.
26. Bressloff, P.C.; Newby, J.M. Stochastic models of intracellular transport. *Rev. Mod. Phys.* **2013**, *85*, 135. [CrossRef]
27. Fedotov, S.; Korabel, N.; Waigh, T.A.; Han, D.; Allan, V.J. Memory effects and Lévy walk dynamics in intracellular transport of cargoes. *Phys. Rev. E* **2018**, *98*, 042136. [CrossRef]
28. Korabel, N.; Han, D.; Taloni, A.; Pagnini, G.; Fedotov, S.; Allan, V.; Waigh, T.A. Local analysis of heterogeneous intracellular transport: Slow and fast moving endosomes. *Entropy* **2021**, *23*, 958. [CrossRef]
29. Han, D.; Alexandrov, D.V.; Gavrilova, A.; Fedotov, S. Anomalous Stochastic Transport of Particles with Self-Reinforcement and Mittag–Leffler Distributed Rest Times. *Fractal Fract.* **2021**, *5*, 221. [CrossRef]
30. Simpson, C.; Yamauchi, Y. Microtubules in influenza virus entry and egress. *Viruses* **2020**, *12*, 117. [CrossRef]
31. Ando, D.; Korabel, N.; Huang, K.C.; Gopinathan, A. Cytoskeletal network morphology regulates intracellular transport dynamics. *Biophys. J.* **2015**, *109*, 1574–1582. [CrossRef]
32. Wannasarit, S.; Wang, S.; Figueiredo, P.; Trujillo, C.; Eburnea, F.; Simón-Gracia, L.; Correia, A.; Ding, Y.; Teesalu, T.; Liu, D.; et al. A virus-mimicking pH-responsive Acetalated dextran-based membrane-active polymeric nanoparticle for intracellular delivery of antitumor therapeutics. *Adv. Funct. Mater.* **2019**, *29*, 1905352. [CrossRef]
33. Braga, C.B.; Kido, L.A.; Lima, E.N.; Lamas, C.A.; Cagnon, V.H.; Ornelas, C.; Pilli, R.A. Enhancing the Anticancer Activity and Selectivity of Goniothalamin Using pH-Sensitive Acetalated Dextran (Ac-Dex) Nanoparticles: A Promising Platform for Delivery of Natural Compounds. *ACS Biomater. Sci. Eng.* **2020**, *6*, 2929–2942. [CrossRef] [PubMed]
34. Figueroa, S.M.; Fleischmann, D.; Goepferich, A. Biomedical nanoparticle design: What we can learn from viruses. *J. Control. Release* **2021**, *329*, 552–569. [CrossRef] [PubMed]
35. Ma, X.Y.; Hill, B.D.; Hoang, T.; Wen, F. Virus-inspired Strategies for Cancer Therapy. *Semin. Cancer Biol.* **2021**. [CrossRef] [PubMed]